Journal of Petroleum Science and Engineering 188 (2020) 106951

Contents lists available at ScienceDirect

Journal of Petroleum Science and Engineering

journal homepage: http://www.elsevier.com/locate/petrol

Organic geochemistry characterization of Late Jurassic bituminous shales and their organofacies and oil generation potential in the Shabwah depression, southeast Sabatayn, Yemen

Mohammed Hail Hakimi [a,*], Adel M. Al-Matary [b], Osama El-Mahdy [c,d], Baleid Ali Hatem [e], Ali Y. Kahal [f], Aref Lashin [c,g]

[a] Geology Department, Faculty of Applied Science, Taiz University, 6803, Taiz, Yemen
[b] Department of Earth and Environmental Sciences, Sana'a University, Sana'a, Yemen
[c] Petroleum and Natural Gas Engineering Department, College of Engineering, King Saud University, Riyadh, 11421, Saudi Arabia
[d] El Menia University, College of Engineering, El Menia, Egypt
[e] Department of Geology, University of Malaya, 50603, Kuala Lumpur, Malaysia
[f] Geology and Geophysics Department, College of Science, King Saud University, Riyadh, Saudi Arabia
[g] Geology Department, Faculty of Science, Benha University, P.O. Box 13518, Benha, Egypt

ARTICLE INFO

Keywords:
Late Jurassic bituminous shales
Organofacies
Oil-generation
Yemen

ABSTRACT

Bituminous shales of the Late Jurassic Madbi Formation from Shabwah depression in the south-eastern Sabatayn Basin has been collected and analyzed. The organofacies, paleo-sedimentary environmental conditions and oil generation potential are discussed based on combined geochemistry and petrology investigations. Biomarkers indicate that the bituminous-analyzed shales contain mainly marine phytoplankton algae and minor land plants and deposited under reducing environmental conditions. The rich in lipids from phytoplankton algae and land plants suggest high Type II to mixtures of Types II and Type III kerogen as the original organic facies during deposition. This is consistent with significant amounts of alginite and amorphous organic matter, with minor vitrinite land plants observed under microscope and hydrogen index (HI) values of 210–679 mg HC per g TOC and indicated good to excellent oil-source rocks. The presence of the reducing conditions during deposition consequently enhanced the preservation and subsequently gave rise to enrichment of organic matter in the analyzed bituminous shale as indicated by the relatively high TOC values between 1 and 14 wt%.

The geochemical maturity indicators show that the analyzed bituminous shales have reached a low maturity stage, and commercial oils have not yet generated. Therefore, the results presented and discussed in this study suggest that the low maturity bituminous shales can be heated to crack the kerogens and subsequently significant amount of oil can be generated. This will lead to a huge alternative potential of unconventional resources and provide a sense of extending the exploration activities for both unconventional and conventional petroleum resources in the whole Basin.

1. Introduction

The Sabatayn Basin is an important oil-preceding basin in the northern central of Yemen, which it has attracted unprecedented attention by petroleum industries and academic researchers (Brannin et al., 1999; Csato et al., 2001; Alaug et al., 2011; Hakimi and Abdullah, 2013a; Hakimi et al., 2014; Hakimi and Ahmed, 2016; Al-Areeq et al., 2018). The conventional petroleum exploration in the Sabatayn Basin began long time, since many surface oil seeps and oils have been recognized at many locations in the basin (SPT, 1994; Hakimi and Abdullah, 2013a and b; Hakimi et al., 2019a). In the last 20 years, the hydrocarbon exploration activity in the north-west part of the Sabatayn Basin (Marib-Al-Jawf sub-basins) focus mainly on organic-rich shales within the Late Jurassic units i.e., Safer, Lam and Meem members, which are regionally represented throughout the Sabatayn Basin (e.g. SPT, 1994; Brannin et al., 1999; Csato et al., 2001). Extensive geochemical,

* Corresponding author.
E-mail address: ibnalhakimi@yahoo.com (M.H. Hakimi).

https://doi.org/10.1016/j.petrol.2020.106951
Received 19 July 2019; Received in revised form 28 November 2019; Accepted 9 January 2020
Available online 10 January 2020

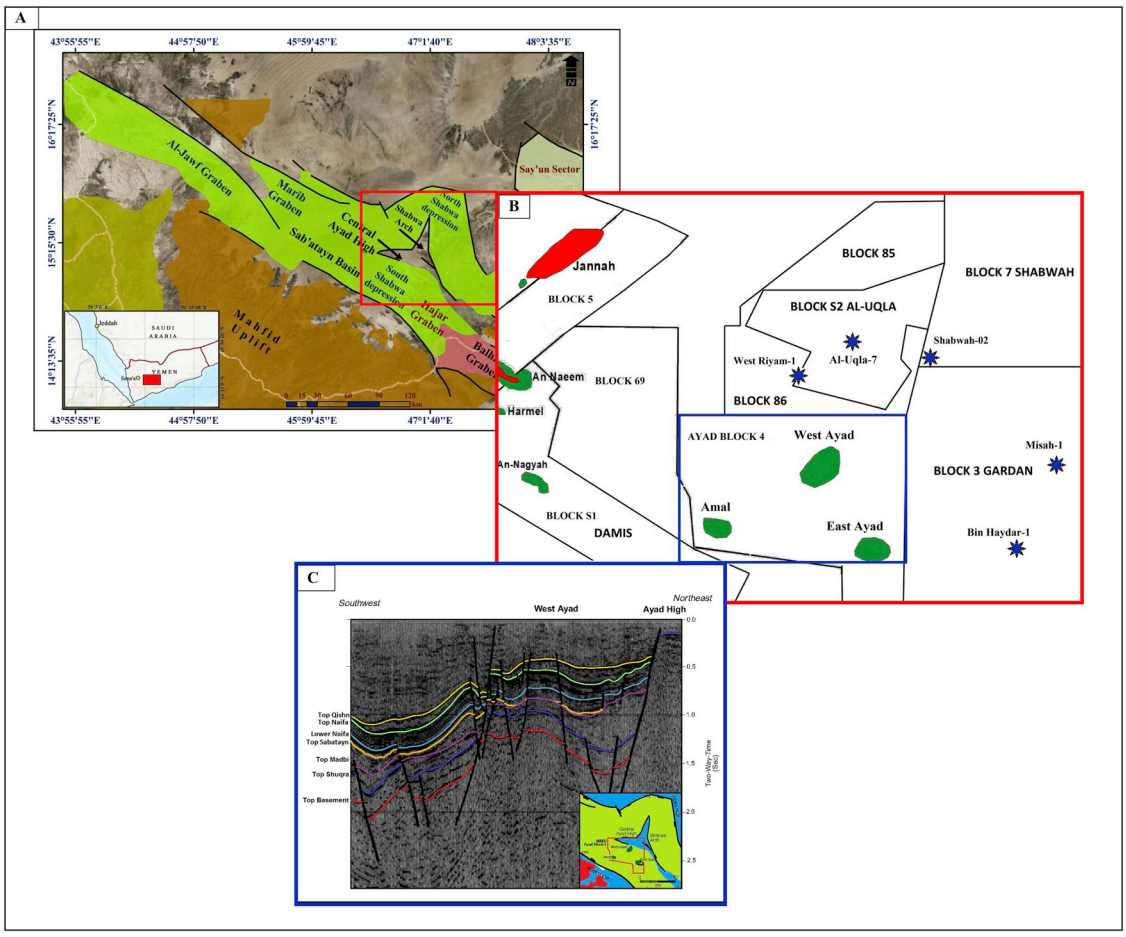

Fig. 1. (A) The main sub-basins (e.g., Al-Jawf, Marib, and Hajar): and the Shabwah depression in the Sabatayn rift system basin, Yemen. (B) Location map of exploration blocks in the Shabwah depression including the studied wells. (C) Structural cross-section across Ayad oilfields, showing the main structural types in the Shabwah depression.

organic petrological and basin modeling studies have been performed on the Late Jurassic units i.e. Lam, Meem and Safer members in the north-west part of the Sabatayn Basin, and showed that theses organic-rich shales are highly promising source rocks for conventional petroleum exploration and development (Alaug et al., 2011; Hakimi and Abdullah, 2013a and b; Hakimi et al., 2014; Hakimi and Abdullah, 2015). The Lam and Meem shales in the flanks of the basin possess higher thermal maturity than the safer member (Hakimi and Abdullah, 2013a; Hakimi et al., 2014), and are considered to be the main source rocks for oil and gas prone, with high amounts of gas contributing from the Meem unit (Hakimi et al., 2014, 2019b). Recently, the conventional reserve in the Sabatayn Basin is declining, thus, unconventional petroleum exploration increased significantly and the exploration and drilling activity is looking for unconventional petroleum resources from the Late Jurassic bituminous shales in the structural high areas in the northern part of the Sabatayn Basin, where they are at most lower maturity stage (e.g. Hakimi et al., 2018). In the current study, the organofacies and oil-generation potential of the bituminous shales in the Late Jurassic Madbi Formation that exposed in the Shabwah depression of southern Sabatayn Basin were documented using multi geochemical analyses, including content of organic carbon (TOC), Rock-Eval pyrolysis and biological markers as well as study the organic facies under microscope. This study, in addition to previous findings on the Late Jurassic bituminous shales in the northern part of the Sabatayn Basin (e.g. Hakimi et al., 2018) would be enhanced exploration interest related to unconventional petroleum exploration in the areas, extending from north-western to south-eastern Sabatayn Basin. Any new information can ascertain prediction of different types of petroleum resources that can consequently lead to increase of unconventional as well as conventional petroleum resource discovery in the whole basin.

2. Geological background

The Sabatayn Basin extends from the north-western to south-eastern of Yemen, which includes three grabens (i.e. Al-Jawf, Marib and Hajar) and on depression (i.e. Shabwah) as shown in Fig. 1A. This basin is initially formed during late Jurassic and related to the breakdown of the Mesozoic deposits from the Gondwana during early Kimmeridgain to early Berriasian (Redfern and Jones, 1995; As-Saruri et al., 2010). The Mesozoic rift system has several normal faults, whereby developed from the underlying faults that formed during late Jurassic (Fig. 1C).

The Shabwah depression is belonging to southeastern Sabatayn Basin (Fig. 1A), and filled by a thick Mesozoic sedimentary sequence of the Jurassic to Cretaceous age, followed by the Paleocene sediments (Fig. 2). This stratigraphic sequence was controlled by tectono-stratigraphic i.e. pre-, syn- and post-rifts, and are controlled by mainly marine and subordinate continental depositional environments (Beydoun et al., 1998).

The middle Jurassic Kuhlan Formation is consisted mainly of major sandstones and subordinate conglomerates, mudstones and limestone beds that rest unconformably over the Precambrian basement rocks (Fig. 2). The Middle-Late Jurassic Shuqra carbonates lie on upper part of the Kuhlan Formation with a conformable contact (Fig. 2), which is further unconformably topped by the syn-rift sediments of Late Jurassic Madbi Formation (Fig. 2). The Madbi Formation comprises of mixed

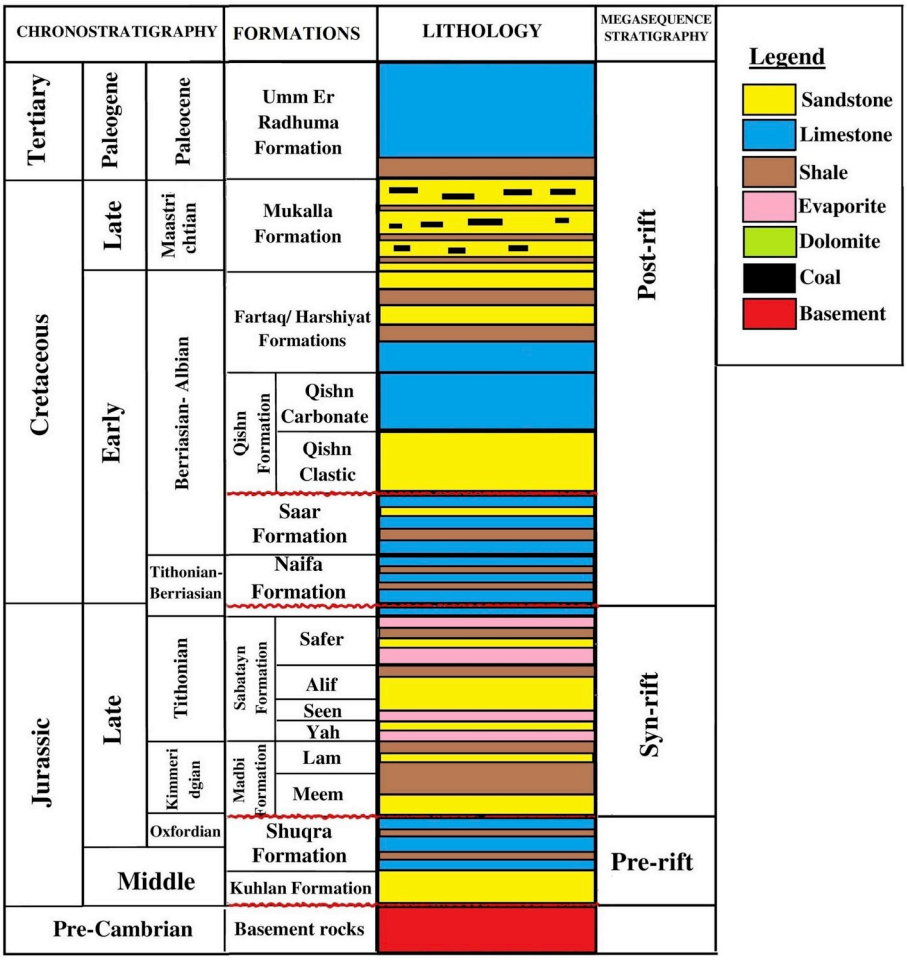

Fig. 2. Generalized stratigraphic column of Pre-Cambrian–Tertiary sequences in the Shabwah depression of southeastern Sabatayn Basin.

shallow marine sandstones, turbidites and fine grained shales that accumulated during the initial rifting in an early Kimmeridgian time. This formation includes organic-rich shale intervals with the Meem and Lam members (Fig. 2), and they are considered as main source rocks in the basin. The organic-rich shales were sampled from the Meem and Lam members in the Shabwah depression of the Sabatyen Basin (Fig. 1B).

The mixed evaporite-clastic sediments of the late Tithonian Sabatayn Formation are conformably covering the Madbi Formation (Fig. 2), and have good sealing characteristics. The thickness of these Salt sediments changes widely in the Sabatyen Basin with a remarkable decrease in order laterally, from the southeast including the Shabwah depression and Hajar graben to northwest, including the northern of the Al-Jawf graben (SPT, 1994). Latest Jurassic-earliest Cretaceous Naifa Formation lie on the Sabatayn Formation (Fig. 2), and composed of mixed carbonate and shale deposits. The Naifa Formation is overlain unconformably by a post-rift sedimentary sequence; both belonging to the Cretaceous-Paleocene age (Fig. 2). A post-rift sequence composed of mixed clastic and carbonate sediments is well represented in the area by the deposits of the upper Naifa, Saar, Qishn, Fartaq/Harshiyat, Mukalla and Umm Er Radhuma formations (Fig. 2).

3. Sampling and analytical procedures

In total, 84 representative samples were obtained from five exploration wells (Misah-1, Bin Haydar-1, West Riyam-1, Al-Uqlah-7 and Shabwah-02) in the Shabwah depression of south-eastern Sabatayn Basin (Fig. 1). The analyzed samples are represented by the bituminous shales within the Late Jurassic Madbi members i.e. Lam and Meem (Fig. 2).

The samples were grinding to fine particles and subsequently were pre-treated using HCl acid to remove carbonates from the whole rock prior to the analysis organic carbon content. The mount of organic matter (TOC) was determined using a LECO CS-125 equipment. The powdered samples were further analyzed using Rock-Eval pyrolysis analysis and subjected to character source rock. The bulk pyrolysis process measured several geochemical parameters such as a free petroleum (S_1, mg/g), total petroleum yield from cracking of kerogen (S_2, mg/g) and oven temperature at maximum S_2 generation (T_{max}) (Table 1). The measured TOC Rock-Eval yields i.e. S_1 and S_2 were further used in calculating several geochemical parameters such as hydrogen index (HI= S_2*100/TOC), petroleum yield (PY=S_1+S_2) and production index (PI= S_1/S_1+S_2) (Table 1).

For bitumen extraction, mixture solvents of dichloromethane (DCM) and methanol (CH_3OH) were used to extract the bitumen (S_1) from 10 powdered samples and carried out using Soxhlet apparatus for 72 h. The saturated, aromatic and polar fractions of the bitumen extracts were fractionated using liquid column chromatography. Gas chromatography–mass spectrometry (GC–MS) experiment was conducted on the saturated fraction using HP 5975B MSD and Finnegan 4000 MS. The temperature of FID gradually increases from 40 °C to 300 °C at a consent rate of 3–4 °C/min, and then was held for 30 min at 320 °C. Peak identification of the biomarker compounds and their related parameters were accomplished on the basis of retention times and mass spectra of the monitored ions of pervious published works of Philp (1985), Peters et al. (2005) and Hakimi et al. (2012), as well as the ratios calculated from peak heights.

For visual kerogen analysis, several dark shale samples were crushed

Table 1
Rock Eval pyrolysis and TOC content data and additional calculated parameters for the oil shale samples in the Late Jurassic Madbi Formation from five wells (Misah-1, Bin Haydar-1, West Riyam-1, Al-Uqlah-7 and Shabwah-02) in the Shabwah depression (SE Yemen).

Blocks	Wells	Depth (MD)	TOC wt.%	Rock-Eval pyrolysis					
				S_1 (mg/g)	S_2 (mg/g)	T_{max} (°C)	HI (mg/g)	PY (mg/g)	PI (mg/g)
BLOCK 3 (GARDAN)	**Misah-1**	2506	1.00	0.30	2.26	442	226	2.56	0.12
		2534	1.20	0.50	2.62	443	218	3.12	0.16
		2546	2.00	0.89	4.21	442	210	5.10	0.17
		2554	2.10	0.90	4.92	445	234	5.82	0.15
		2566	1.70	0.62	4.12	444	242	4.74	0.13
		2574	2.40	0.72	6.00	445	250	6.72	0.11
		2586	2.00	0.69	5.00	445	250	5.69	0.12
		2594	2.10	0.59	5.92	445	282	6.51	0.09
		2606	2.75	0.89	8.40	445	306	9.29	0.10
		2613	2.70	0.75	8.89	443	329	9.64	0.08
		2621	3.60	0.80	12.72	443	353	13.52	0.06
		2628	2.40	0.65	8.67	442	361	9.32	0.07
		2640	3.20	1.10	12.80	443	400	13.90	0.08
		2651	2.90	1.50	12.31	442	425	13.81	0.11
		2659	2.10	0.80	8.58	443	409	9.38	0.09
		2670	2.70	0.70	11.25	442	417	11.95	0.06
		2677	3.30	1.60	13.49	444	409	15.09	0.11
		2689	4.50	2.10	17.68	445	393	19.78	0.11
		2696	4.90	2.30	18.47	446	377	20.77	0.11
		2708	3.20	1.00	11.84	446	370	12.84	0.08
	Bin Haydar-1	2571	1.30	2.70	4.58	434	352	7.28	0.37
		2587	3.10	1.80	12.30	434	397	14.10	0.13
		2597	1.20	0.80	3.69	435	307	3.69	0.18
		2608	1.60	1.10	7.57	436	473	8.67	0.13
		2618	2.80	1.70	10.58	439	378	12.28	0.14
		2623	3.90	2.40	17.46	436	448	19.86	0.12
		2633	7.40	4.70	28.42	440	384	33.12	0.14
		2644	2.30	1.40	7.37	440	321	8.77	0.16
		2659	5.00	3.80	23.02	439	460	26.82	0.14
		2664	8.10	5.00	35.75	445	441	40.75	0.12
		2674	3.40	1.90	13.92	444	410	15.82	0.12
		2680	6.80	4.50	23.96	440	352	28.46	0.16
		2685	5.50	5.00	23.57	436	429	28.57	0.17
		2695	3.90	5.00	17.21	436	441	22.21	0.23
		2710	3.40	2.50	13.49	443	397	15.99	0.16
		2721	2.60	3.60	10.80	445	416	14.40	0.25
		2726	5.20	2.40	20.97	438	403	23.37	0.10
		2731	4.30	2.30	14.88	437	346	17.18	0.13
		2751	3.70	1.90	13.98	447	378	15.88	0.12
		2756	3.30	1.30	9.95	445	302	11.25	0.12
		2772	2.40	0.90	5.61	440	321	6.51	0.14
		2787	2.30	0.80	4.79	439	249	5.59	0.14
		2838	1.30	0.60	3.47	437	217	4.07	0.15
		2848	1.90	0.70	4.14	438	224	4.84	0.14
		2858	2.40	1.3	5.46	438	306	6.76	0.19
		2868	6.50	3.7	8.61	438	211	12.31	0.30
		2883	1.30	1.8	3.60	438	230	5.40	0.33
		2893	2.40	2.2	4.51	439	211	6.71	0.33
		2903	1.90	1.5	4.26	438	236	5.76	0.26
BLOCK S2 (AL-UQLA)	**West Riyam-1**	1844	11.30	9.25	43.52	437	385	52.77	0.18
		1853	7.46	3.39	25.06	439	335	28.45	0.12
		1868	9.36	2.81	35.55	439	379	38.36	0.07
		1878	9.95	2.97	46.29	439	465	49.26	0.06
		1905	1.24	0.45	2.79	439	225	3.24	0.14
		1914	6.83	3.04	30.73	439	450	33.77	0.09
		1923	4.02	1.68	14.36	441	357	16.04	0.10
		1932	2.04	0.64	5.05	441	248	5.69	0.11
		1942	3.44	0.91	11.63	441	338	12.54	0.07
		1951	4.38	1.57	13.15	444	300	14.72	0.11
		1960	10.50	4.59	40.12	440	382	44.71	0.10
		1969	10.45	9.81	44.61	440	427	54.42	0.18
		1981	7.32	4.36	30.20	441	413	34.56	0.13
		1990	5.38	2.88	15.19	442	282	18.07	0.16
		1999	5.11	2.07	15.42	445	302	17.49	0.12
		2009	6.32	3.25	23.83	444	377	27.08	0.12
		2018	7.09	4.50	29.00	444	409	33.50	0.13
		2027	4.06	1.74	13.45	442	331	15.19	0.11
		2036	9.30	6.02	40.54	442	436	46.56	0.13
		2045	5.97	3.40	27.02	443	453	30.42	0.11
		2054	3.68	2.13	13.26	442	360	15.39	0.14
		2063	3.56	2.30	11.33	442	318	13.63	0.17
		2073	4.28	2.13	13.02	443	304	15.15	0.14

(*continued on next page*)

Table 1 (*continued*)

Blocks	Wells	Depth (MD)	TOC wt.%	Rock-Eval pyrolysis					
				S_1 (mg/g)	S_2 (mg/g)	T_{max} (°C)	HI (mg/g)	PY (mg/g)	PI (mg/g)
		2082	2.66	1.45	7.78	441	292	9.23	0.16
		2091	2.49	1.49	5.74	438	231	7.23	0.21
		2100	2.30	1.37	5.25	442	228	6.62	0.21
		2131	3.08	1.39	7.71	440	250	9.10	0.15
	Al-Uqlah-7	2534	3.87	2.13	9.70	443	251	11.83	0.18
		2556	3.76	2.10	9.13	437	243	11.23	0.19
		2570	3.30	1.56	7.43	441	225	8.99	0.17
BLOCK 7 (SHABWAH)	**Shabwah-02**	2443	6.46	3.24	21.83	437	338	25.07	0.13
		2446	14.00	–	–	–	–	–	–
		2525	3.91	–	–	–	–	–	–
		2529	10.44	6.96	70.89	442	679	77.85	0.09
		2658	4.43	4.61	14.53	445	328	19.14	0.23

S_1: Volatile hydrocarbon (HC) content, mg HC/g rock TOC: Total organic Carbon, wt%.
S_2: Remaining HC generative potential, mg HC/g rock PI: Production Index = $S_1/(S_1+S_2)$.
T_{max}: Temperature at maximum of S_2 peak PY: Potential Yield = S_1+S_2 (mg/g).
HI: Hydrogen Index = S_2x 100/TOC, mg HC/g TOC.
Eq. VRo (%): Computed VRo from T_{max} = 0.0180 *T_{max} −7.16.

roughly to approximately pea-sized fragments. The visual kerogen analysis was used to identify the organic facies and detect the quality of the organic matter derived from geochemical analysis.

4. Results and discussion

4.1. Kerogen microscopy

In the current study, kerogen microscopy examination using both reflected plane-polarized and ultraviolet (UV) lights was conducted on the analyzed shale samples to identify the organofacies. Based on the optical results, the analyzed samples mainly comprise inorganic materials, which include clay, quartz and pyrite minerals (Fig. 3a-c). These inorganic minerals are mixed with dispersed organic matter such as alginate and amorphous organic matter (AOM) as shown in Fig. 3d-f. Significant quantities of vitrinite with minor amount of inertinite organic matter were also recognized (Fig. 3c), which indicate the input of land plants. The structured organic matter is characterized by a dominance of yellow to greenish fluorescence alginate and AOM (Fig. 3d-f), which is commonly known marine organic matter and named sapropel or sapropelite (Taylor et al., 1998). However, the alginate assemblages are present mainly as telalginite and lamalginite alga (Fig. 3d and e). The dominance of fluorescence alginate and AOM assemblages (Fig. 3d-f) imply high organic facies of Type II kerogen, which is a common organic matter in oil shale that deposited in marine reducing environmental conditions (Tissot and Welte, 1984; Hakimi et al., 2001; Makeen et al., 2015; Hakimi et al., 2016a and b). Additional information concerning the optical features, provide evidence for the presence of the elongated solid bitumen within quartz minerals and clay-rich zones (Fig. 3g and h).

4.2. Richness of organic matter and generative potential

Knowing the amount of organic matter in the analyzed samples and their richness were investigated using both TOC content and pyrolysis results (Peters and Cassa, 1994; Mccarthy et al., 2011) as tabulated in Table 1. Based on the percentage of TOC content, the analyzed samples are originally rich, with high TOC values between 1 and 14 wt % (an average 4.3 wt %). Generally, the analyzed samples have high organic matter within TOCs of more than 2%, however, it is noted that the analyzed samples with TOC percent less than 2 or 1, could be attributed to relatively high terrestrial minerals that diluted the organic matter (Talbot, 1988; Mohialdeen and Hakimi, 2016; Hakimi et al., 2016a and b). However, the enrichment of organic matter in the analyzed bituminous shales is probably demonstrated by oxygen poor conditions during the Late Jurassic time as discussed in the next subsections.

The analyzed samples also exhibited high yields of the free hydrocarbon (*S*1) and total hydrocarbon yield from cracking of kerogen (*S*2), ranging from 0.30 to 9.81 mg HC/g rock and 2.62–70.89 mg HC/g rock, respectively (Table 1). The volume of petroleum would generate during burial thermal was estimated based on both Rock-Eval *S*1 and *S*2 yields (Merrill, 1991; Fatma and Sadettin, 2013), whereby together make up the oil yield potential (PY). According to values of oil yield potential, the analyzed samples range between good and excellent generative potential (Fig. 4A), with PY values between 1.88 and 45.10 mg HC/g rock, and thus higher petroleum generation can be expected in a sufficient maturity level. Moreover, the free hydrocarbons (*S*1) for the analyzed samples is elevated and excessed of more than 9.0 mg/gm in several samples (Table 1). This would be suggested present significant volume of migrated hydrocarbons (Abrams et al., 2017). In this study, the relatively higher *S*2 and total organic carbon (TOC) content compared to the *S*1 suggest that the high *S*1 measured during pyrolysis (Table 1), and the bitumen materials observed under microscope (Fig. 3g and h) are indigenous materials (Fig. 4B). The petroleum potential yield was also inferred from the high amount of bitumen obtained in the extracted organic matter (EOM). The range of the EOM values between 1336 and 9757 ppm (Table 2) is consistent with the moderate to high TOC content and further represents good to excellent characteristics for hydrocarbon generation (Fig. 5). Furthermore, the saturated, aromatic and polar proportions of the extracted bitumen suggest that the analyzed shale samples would generate oils with high paraffinic gradient to naphthenic materials (Fig. 6).

4.3. Bulk kerogen characteristics

The information on the bulk kerogen type are provided from geochemical hydrogen (HI) and oxygen index (OI) values (e.g. Peters and Cassa, 1994; Hunt, 1996). In this study, the Rock-Eval instrument does not measure carbon oxide content (no *S*3 peak), hence, the information on oxygen content is absence and the kerogen type in the analyzed samples was identified only based on hydrogen index (HI) data (Table 1). The analyzed samples have HI values from 210 to 679 mg HC/g TOC, and most of the analyzed samples had significantly high HI values of more than 300 mg HC/g TOC (Table 1). However, the potential of a source rock to generate hydrocarbon is usually determined by its hydrogen index (HI) rather than oxygen index (OI), because the oxygen index is not accurate due to the combination of oxygen that was released from organic matter with that from carbonate or from oxidation of kerogen (Tissot and Welte, 1984; Espitalié et al., 1985; Mukhopadhyay et al., 1995). In this respect, the analyzed bituminous shale samples

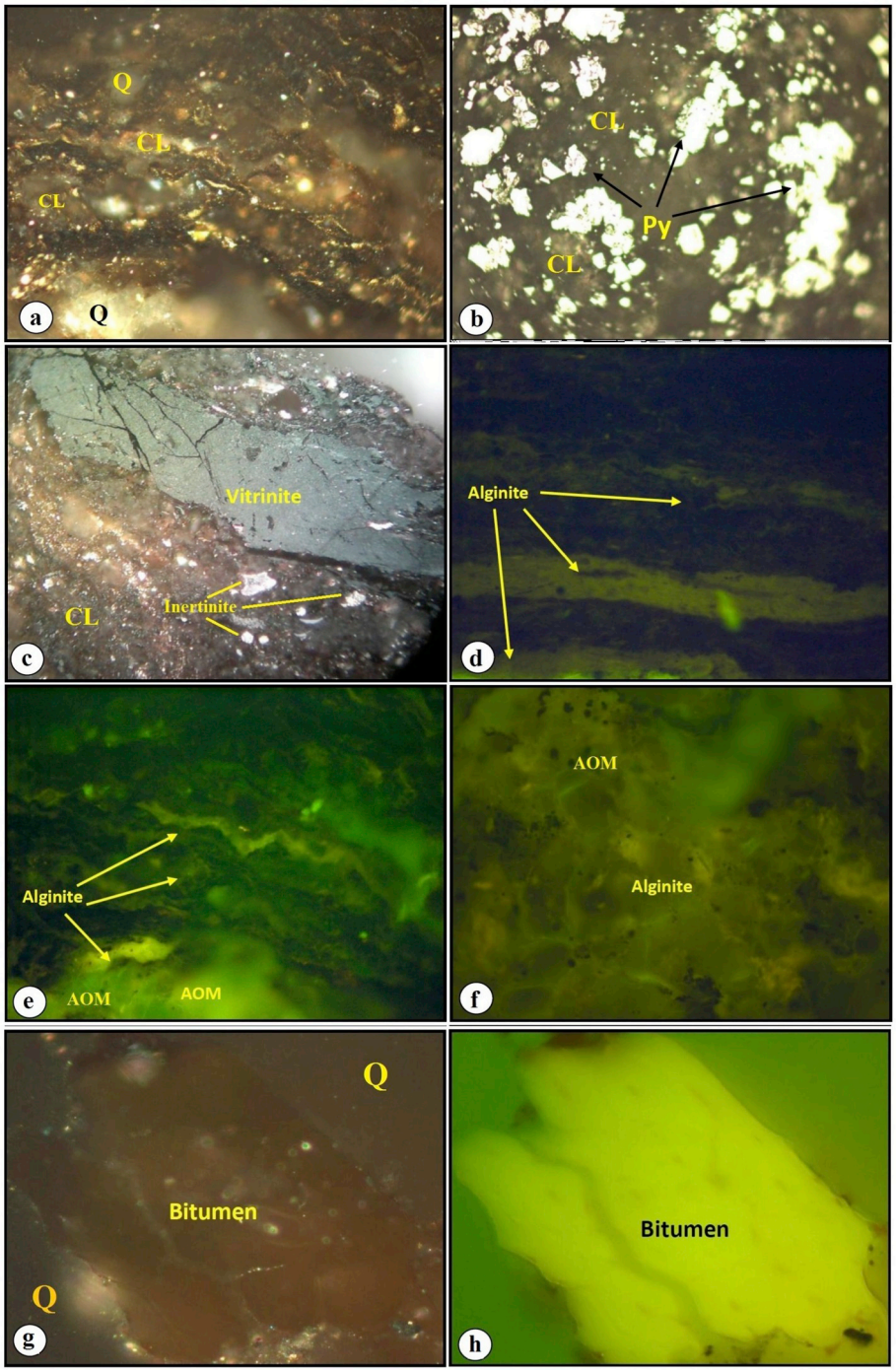

Fig. 3. Photomicrographs of inorganic and organic materials from the analyzed bituminous shale samples in the Shabwah depression as shown under reflected light (a)–(c) and under ultraviolet (UV) light (b)–(f), with a field width of 0.2 mm. (a), (b) Inorganic materials including clay (CL), quartz (Q), and pyrite (Py); (c) terrigenous organic matter including vitrinite and inertinite assemblages; (d), (f) alginite assemblages including telalginite and lamalginite associated with amorphous organic matter (AOM); (g) Elongated clay zone filled with solid bitumen and (h) view of (a) under UV light showing yellow fluorescence of solid bitumen.. (For interpretation of the references to colour in this figure legend, the reader is referred to the Web version of this article.)

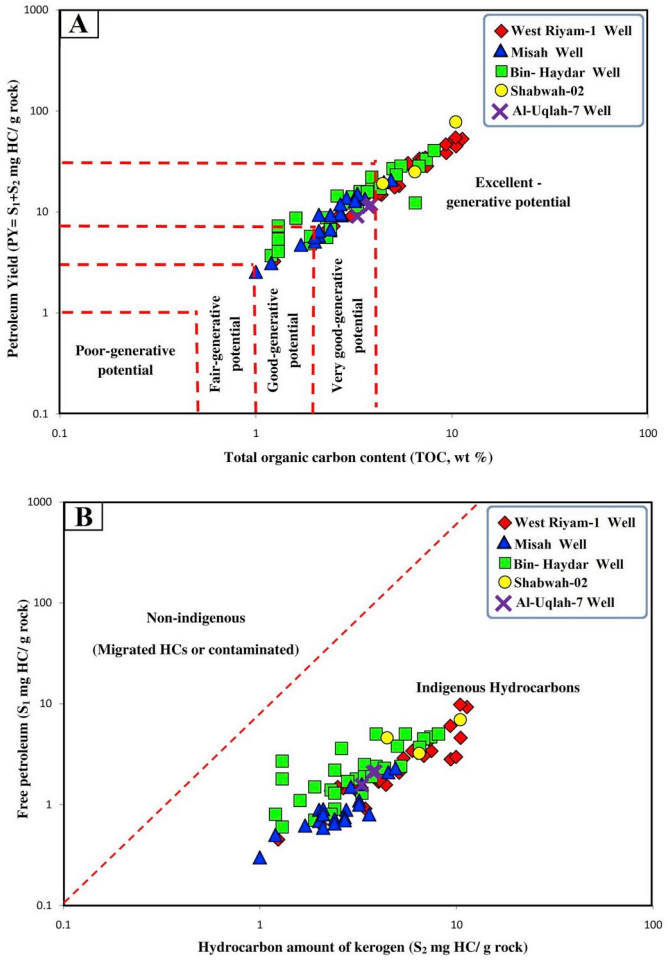

Fig. 4. Cross-plots of geochemical results of (A) total organic carbon (TOC) content versus petroleum yield (PY) and (B) total organic carbon (TOC) content versus pyrolysis yield (S_1) for the analyzed bituminous shale samples in the Shabwah depression.

contain a dominant of Type II kerogen, with a minor organic facies of Type I and II/III as illustrated in the modified Van Krevelen diagram of HI and Tmax plot of Fig. 7A. The *S*2 and TOC diagram further confirms the Type II organic facies is a major kerogen component in the analyzed samples, with a minor Types II-III and I kerogen, respectively (Fig. 7B). In addition, the modified Van Krevelen diagram shows that the organic facies in the analyzed bituminous shale samples is at low maturity level, corresponding to early-mature to moderate mature (Fig. 7B) as clearly indicated from Tmax values of 434–447 °C (Table 1). In concordance with previous Tmax data, the production index (PI) was also used to assess the maturation of organic matter in the analyzed samples. The presence of low to relatively high of PI values is further suggest that the analyzed samples in the entire Shabwah depression are at early mature to peak mature for oil window generation as clearly agreement with Tmax data (Fig. 8).

4.4. Biomarker characteristics

The specific ratios and parameters derived from the biomarker distributions of the 10 analyzed bituminous shale samples in West Riyam-1 and Al-Uqlah-7 wells are shown in Table 2. The most biomarkers extracted from the saturated fraction of the analyzed samples were derived from the GC chromatograms and mass fragmentograms of the m/z 191 and m/z 217 ions (Fig. 9), and include *n*-alkanes, acyclic

Table 2
Organic geochemical results of the selected oil shale in tow well (West Riyam-1 and Al-Uqlah-7) in the Shabwah depression (SE Yemen); including bitumen extracted and specific biomarker parameters and ratios.

Blocks	Wells	Depth (m)	EOM (ppm)	Fractions (wt. %)				*n*-alkane and isoprenoids				Triterpanes and terpanes (m/z191)			Steranes (m/z217)			
				Sat.	Aro.	HC	polar Non-HC	Pr/Ph	Pr/C_{17}	Ph/C_{18}	CPI	C_{29}/C_{30}	G/C_{30}	HCR_{31}/HC_{30}	C_{27}/C_{29} Regular steranes	Regular steranes (%)		
																C_{27}	C_{28}	C_{29}
BLOCK S2 (AL-UQLA)	**West Riyam-1**	1844	9757	42.56	15.41	57.97	42.03	1.07	0.82	0.96	1.02	0.43	0.27	0.25	1.08	39.99	22.84	37.17
		1878	7531	37.59	15.42	53.01	46.99	1.34	0.79	0.67	1.02	–	–	–	–	–	–	–
		1923	4290	42.99	13.51	56.50	43.50	1.33	0.71	0.65	1.00	0.45	0.14	0.32	0.71	32.16	22.24	45.60
		1969	6887	58.08	13.71	71.79	28.21	1.46	0.80	0.67	1.02	0.36	0.07	0.32	0.79	34.02	23.08	42.90
		2018	4780	49.96	15.89	65.85	34.15	1.30	0.85	0.78	1.01	0.42	0.07	0.27	0.84	36.49	20.08	43.44
		2063	2259	50.48	17.46	67.94	32.06	1.36	0.59	0.54	1.06	0.37	0.10	0.29	0.89	39.68	15.87	44.44
		2100	1336	56.27	17.20	73.47	26.53	1.41	0.73	0.59	1.05	–	–	–	–	–	–	–
	Al-Uqlah-7	2534	1544	37.43	33.54	70.97	29.01	0.91	0.64	0.63	1.00	0.64	0.08	0.28	1.33	48.48	15.15	36.36
		2556	5634	37.94	42.56	80.50	19.48	1.04	0.86	0.84	1.02	0.63	0.07	0.24	1.12	37.37	29.29	33.33
		2570	3390	38.14	28.86	67.00	32.99	1.05	0.54	0.56	0.97	0.46	0.12	0.26	0.86	37.76	18.37	43.88

Sat.– Saturated hydrocarbons; Aro.– Aromatic hydrocarbons; Non HC– Non-hydrocarbon fractions; HC–Hydrocarbon fractions (Saturated + Aromatic); EOM – Bitumen extraction and chromatographic fractions (ppm of whole rocks).
Pr – Pristane; Ph – Phytane; CPI – Carbon preference index (1): $\{2(C_{23} + C_{25} + C_{27} + C_{29})/(C_{22} + 2[C_{24} + C_{26} + C_{28}] + C_{30})\}$; C_{29}/C_{30}: C_{29} norhopane/C_{30} hopane.
HCR_{31}/HC_{30}: C_{31} regular homohopane/C_{30} hopane; G/C_{30}: Gammacerane index = Gammacerane.C_{30} hopane.

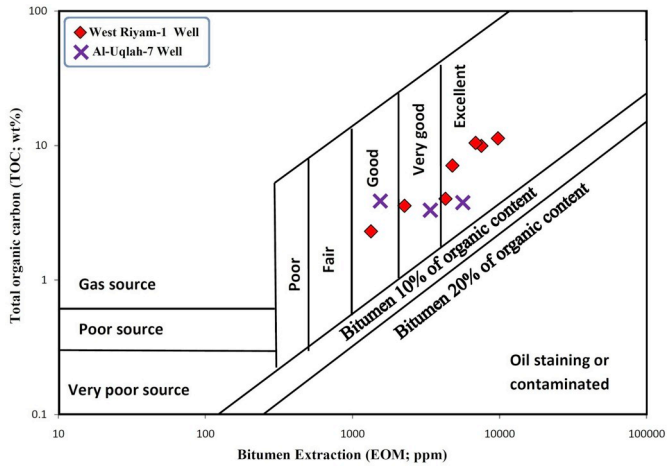

Fig. 5. Cross-plots of geochemical results of total organic carbon (TOC) content versus extractable bitumen for the analyzed bituminous shale samples in the Shabwah depression.

isoprenoids, hopanes, terpanes and steranes. Normal alkane and acyclic isoprenoid distributions show unimodal distribution of abundant low to middle molecular-weight *n*-alkanes (C12–C20) and long-chain *n*-alkane (+*n*-C_{25}) molecular weight compounds (Fig. 9). The *n*-$C_{23\text{-}30}$ distributions in the analyzed samples yielded carbon preference index (CPI) values generally near to 1.0, at a range of 0.97–1.06 (Table 2).

Of the acyclic isoprenoids, pristane (Pr) was more abundant than phytane (Ph) in most of the analyzed samples (Fig. 9). The Pr/Ph ratios were relatively low between 0.91 and 1.46 (Table 2). The isoprenoid ratios of Pr/*n*-C_{17} and Ph/*n*-C_{18} are also calculated from the amounts of isoprenoid compared with *n*-alkanes (C_{17}-C_{18}), resulting relatively low values and range from 0.54 to 0.86 and 0.54–0.96, respectively (Table 2).

In the analyzed samples, the hopanes and terpanes were also identified using *m/z* 191 mass fragmentograms (Fig. 9). *M/z* 191 mass fragmentograms show high abundance of hopanes in all analyzed samples (Fig. 9). However, the C_{30} hopanes are dominant over C_{29}

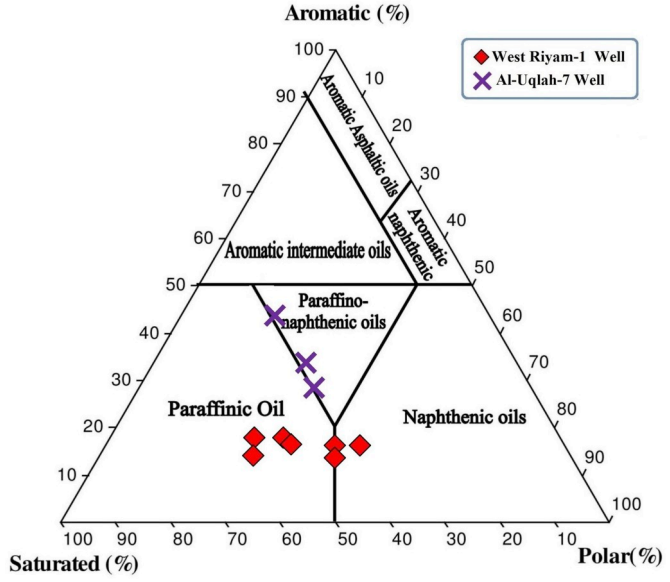

Fig. 6. Ternary diagram of bitumen composition derived from the analyzed bituminous shale samples, showing the petroleum potential class to be generated during burial thermal maturation.

norhopanes (Fig. 9), with relatively low values of C_{29} norhopane/C_{30} hopane ratio of 0.36–0.64 (Table 2). The lower values of C_{29}/C_{30} ratio are typically indicative clay-rich facies (Gürgey, 1999). In particular, the homohopanes are dominated mainly by C_{31}, and the content decreases gradually as carbon content increases in all samples (Fig. 9). The C3122R homohopane/C_{30} hopane (C_{31}R/C_{30}H) ratios range from 0.24 to 0.32 (Table 2), which generally indicates a marine environment of deposition for analyzed shale samples (Hakimi et al., 2012). In addition, the gammacerane are also principally recorded in low quantities in m/z 191 mass fragmentograms for the most analyzed samples (Fig. 9), and its index of gammacerane/C_{30}hopane (G/C_{30}) ranged from 0.07 to 0.27 (Table 2).

The mass fragmentograms of *m/z* 217 show high abundance of steranes and diasteranes in the analyzed samples (Fig. 9). The distributions of homologous series of C_{27}-C_{29} regular sterane in the *m/z* 217 mass fragmentogram of the analyzed samples are characterized by relatively high abundance of C_{27} (32.16–48.48) and C_{29} (33.33–45.60%) regular steranes compared with C_{28} (15.15–29.29%) regular sterane, with averages of 38.24%, 20.87%, and 40.89%, respectively. Thus variable C_{27}/C_{29} sterane ratios were obtained in the range of 0.71–1.33 (Table 2).

4.5. Nature of organic matter and paleo-sedimentary environmental conditions

The previous results presented in the subsections hold the viewpoint of the presence of high bioproductivity of phytoplankton alga in the analyzed bituminous shale from the Shabwah depression that were deposited under a marine reducing environmental conditions. The evidence primarily focused on the organofacies characteristics as observed under the microscope, which are characterized by predominantly marine phytoplankton alga i.e. telalginite and lamalginite and AOM (Fig. 3d-f), with minor contributions of terrigenous land plants i.e., vitrinite (Fig. 3c). The high concentrations of organic matter derived from algal microbial mats i.e. telalginite and lamalginite (Fig. 3d-f) suggest a reducing environmental conditions (Taylor et al., 1998), and thus represents excellent condition for organic matter preservation and enrichment. In addition, the short to medium chain *n*-alkanes (n-C14–n-C23) are frequently present in all analyzed samples (Fig. 9), further suggest a high significant aquatic-derived organic matter (Tissot and Welte, 1984; Peters et al., 2005; Cranwell, 1977; Brassell et al., 1978). This interpretation is also indicated from specific biomarker ratios and parameters such as CPI and isoprenoids (Table 2). High abundance of marine organic matter input during deposition is also achieved from the relation between the CPIs and isoprenoid ratio (Fig. 10A). Furthermore, the lower values of Pr/*n*-C17 and Ph/*n*-C18 ratios are also supported higher contributions of marine aquatic algae and microorganisms, depositing under relatively reducing environmental conditions (Fig. 10B). This relatively low oxygen bottom water condition during deposition consequently enhanced the preservation and subsequently gave rise to enrichment of organic matter as confirmed from the relatively high TOCs of more than 2 wt% (Fig. 4A).

The homologous series of C27-C29 regular sterane in the *m/z* 217 ion are also wieldy used to infer the source of organic matter input (Huang and Meinschein, 1979; Waples and Machihara, 1991). Huang and Meinschein (1979) reported that the regular steranes of C27 and C28 are mainly sourced from the aquatic organic matter i.e., algae and phytoplankton, while C29 regular sterane is typically derived from land plants. In this study, the higher C29 and C27 than C28 regular sterane is well-documented with the distribution of the regular steranes, reflecting an accumulation of mixed organic matter, with high abundance of phytoplankton algae (Fig. 11). This is consistent with high contributions of Types II kerogen and II/III kerogen that obtained from both chemical and optical results (Figs. 3 and 7). This is further underscored by the presence of very low tricyclic terpane concentration in the m/z 191 mass fragmentograms (Fig. 9). The C3122R homohopane/C30 hopane

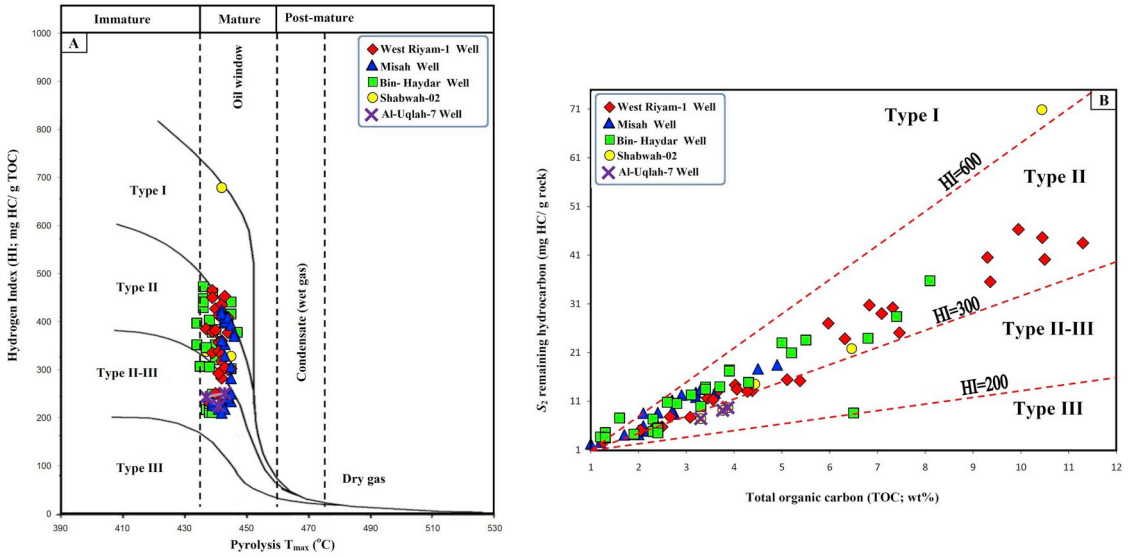

Fig. 7. Characteristics of kerogen based on (A) Rock-Eval hydrogen index (HI) versus T_{max} and (B) total organic carbon (TOC) content versus pyrolysis yield (S_2), showing mainly Type II kerogen with Type II–III and I kerogens in the analyzed bituminous shale samples in the Shabwah depression.

(C31R/C30H) ratios of more than 0.25 indicate that marine organisms are the main biological sources during deposition of these organic-rich sediments (Fig. 12).

The content of acyclic isoprenoids i.e. pristane (Pr) and phytane (Ph) are usually used to assess the origin of organic matter input and paleo-redox environmental conditions during deposition (Didyk et al., 1978; Chandra et al., 1994; Escobar et al., 2011). The Pr/Ph ratios of the analyzed samples are relatively low in the range of 0.91–1.46, reflecting low oxygen bottom water (reducing) conditions. The relation between the Pr/C_{17} and Ph/C_{18} ratios further suggests reducing environmental conditions (Fig. 10B). It is noticeable that the presence of high proportions of framboidal pyrite in the analyzed bituminous shales (Fig. 3b). The pyrite in a framboidal form associated with organic matter that is likely formed as results of converted a reactive iron to pyrite in low oxygen concentrations (Leventhal, 1987). Moreover, the low concentration of gammacerane in m/z 191 mass fragmentograms (Fig. 9), and gammacerane/C_{30} hopane (G/C_{30}) ratios of less than 0.27 (Table 2) suggests a brackish water environment and occur stratified water column. However, the accumulation of organic matter is also believed to be related to tectonics governing the rift basin. The Madbi Formation, including the bituminous shales in this study were accumulated during the initial rift activity in the early Kimmeridgian, and continued until the late Tithonian in synchronicity with the Gondwana breakup (Redfern and Jones, 1995; As-Saruri et al., 2010). Thus, large rift graben area in the Shabwah depression restricted the input of land plants and promoted to accumulate aquatic organisms in the bituminous shales as indicated by their biomarkers and organofacies characteristics obtained from geochemical and microscopy results. Moreover, the restricted water circulation in the rift graben contributed to good preservation of organic matter that consequently enhanced organic richness as evidenced by the presence of a stratified water column and the relatively reducing environmental conditions during deposition of these bituminous rocks in Late Jurassic time.

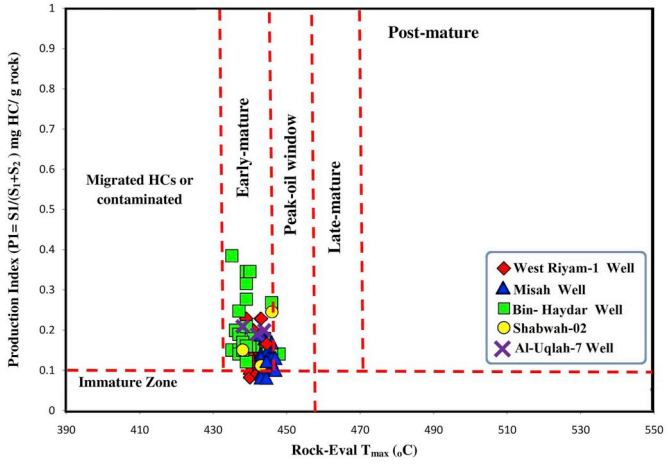

Fig. 8. Cross-plots of Rock-Eval pyrolysis T_{max} versus production index (PI), indicating that the analyzed bituminous shale samples are early-mature source rocks in the oil generation window.

4.6. Oil generation potential and contribution to unconventional petroleum resources

In this study, the petroleum generation potential (oil and/or gas) during maturation was evaluated based on the organofacies characterization and type of kerogen in the analyzed samples. However, the organic facies in the analyzed samples was identified using both chemical and optical results. Accordingly, the organic facies types are characterized by predominately Type II kerogen and mixtures of II and III kerogens, with a minor Type I kerogen (Fig. 5) as confirmed by their pyrolysis HI values between 210 and 679 mg HC per g TOC (Table 1). This is good agreement with high abundance of fluorescent sapropelic materials (i.e. alginate and AOM), with minor land plants (vitrinite). The high contributions of alginate organic matter are consistent with predominantly Types I and II kerogen, with their hydrogen index values of more than 300 mg HC per g TOC. Meanwhile, the analyzed samples have significant amount of AOM and vitrinite land plants are characterized by high significance of a mixtures of II and III kerogens, and HIs of less than 300 mg HC per g TOC. The abundant of Type I and II kerogens suggests the dominant presence of aquatic-derived organic matter i.e. phytoplankton algae, and are of marine origin that was deposited under reducing environmental conditions (Taylor et al., 1998; Hakimi et al., 2001; Hakimi et al., 2016a). However, the hydrogen-rich Type I and II kerogens that were obtained in the analyzed bituminous shales would generate mainly liquid hydrocarbons i.e. oil (Fig. 13).

To improve the understanding of the oil shale and/or shale oil resources to aid petroleum exploration in the Shabwah depression, the current study reveals a relatively low maturity level of the analyzed samples (Fig. 8), thus, they were not enough heated to reach peak oil-

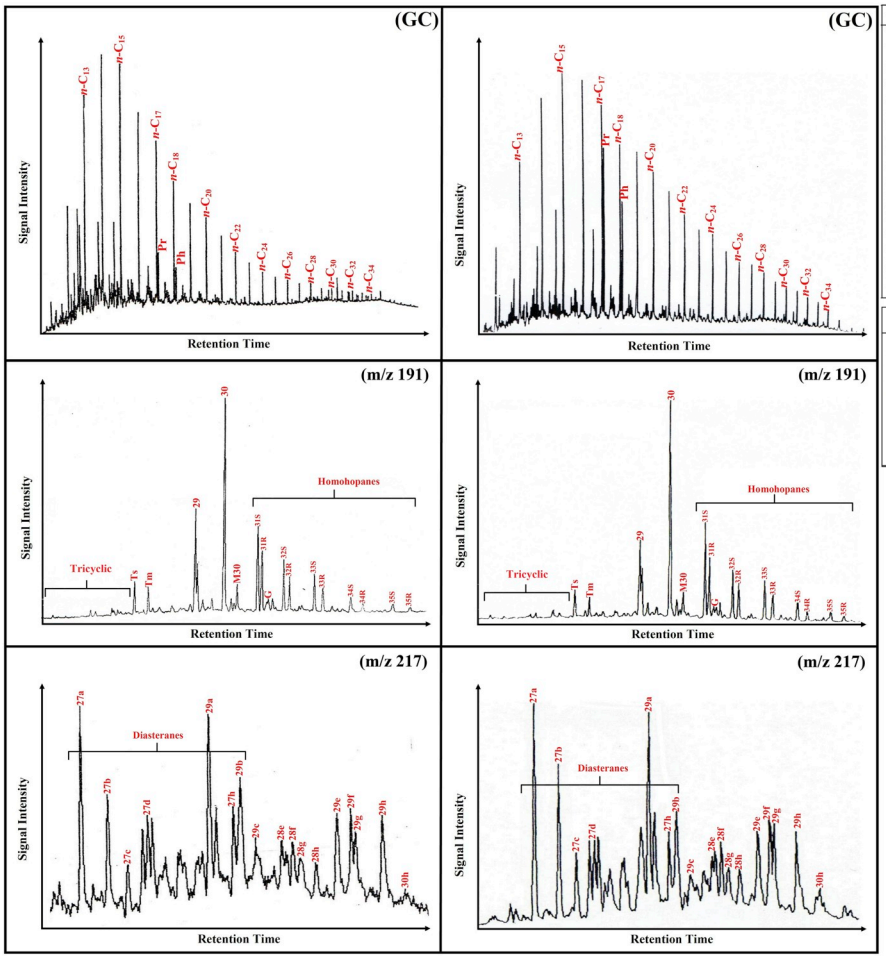

(I) Peak *no.*	Compound abbreviation	(m/z 191)
Ts	18α(H),22,29,30-trisnorneohopane	Ts
Tm	17α(H),22,29,30-trisnorhopane	Tm
29	17α,21β(H)-nor-hopane	C_{29} hop
29M	17β(H),21α(H)-hopane (moretane)	C_{29}Mor
30	17α,21β(H)-hopane	Hopane
30M	17 β,21α (H)-Moretane	C_{30}Mor
31S	17α,21β(H)-homohopane (22S)	C_{31}(22S)
31R	17α,21β(H)-homohopane (22R)	C_{31}(22R)
32S	17α,21β(H)-homohopane (22S)	C_{32}(22S)
32R	17α,21β(H)-homohopane (22R)	C_{32}(22R)
33S	17α,21β(H)-homohopane (22S)	C_{33}(22S)
33R	17α,21β(H)-homohopane (22R)	C_{33}(22R)
34S	17α,21β(H)-homohopane (22S)	C_{34}(22S)
34R	17α,21β(H)-homohopane (22R)	C_{34}(22R)
35S	17α,21β(H)-homohopane (22S)	C_{35}(22S)
35R	17α,21β(H)-homohopane (22R)	C_{35}(22R)

(II) Peak *no.*	Compound abbreviation	(m/z 217)
a	13β,17α(H)-diasteranes 20S	Diasteranes
b	13β,17α(H)-diasteranes 20R	Diasteranes
c	13α,17β(H)-diasteranes 20S	Diasteranes
d	13α,17β(H)-diasteranes 20R	Diasteranes
e	5α,14α(H), 17α(H)-steranes 20S	ααα20S
f	5α,14β(H), 17β(H)-steranes 20R	αββ20R
g	5α,14β(H), 17β(H)-steranes 20S	αββ20S
h	5α,14α(H), 17α(H)-steranes 20R	ααα20R

Fig. 9. Mass fragmentograms of GC, m/z 191, and m/z 217 for the saturated hydrocarbon fractions of two analyzed bituminous shale samples.

generation window. Therefore, these relatively low mature bituminous rocks can be heated to crack the kerogens that will subsequently generate significant oils, thus, an alternative unconventional oil-shale exploration is recommended. However, the geochemical results in this study have highlighted an important finding of the late Jurassic shale rocks that possess potential to act as unconventional resource deposits. Thus, in collaboration with the high thickness (200–300 m) of the bituminous rocks this would be expected of huge oil resources and enhanced exploration interest related to unconventional petroleum exploration that can consequently lead to increase of unconventional as well as conventional petroleum resource discovery in the whole Sabatayn Basin.

5. Conclusions

A compilation of organic geochemical and petrological investigations was performed on 84 bituminous shale samples in the Late Jurassic Madbi Formation from five wells in the Shabwah depression (SE Yemen). The results of this study give strong conclusions as highlighted below:

1 The bituminous shales within the Late Jurassic Madbi Formation are organically rich and have high TOC content between 1 and 14 wt %, indicating good to excellent source rocks potential.

2 Marine organic matter is mainly occur in the analyzed bituminous shales and is dominated by phytoplankton algae. Lower contributions to the organic matter from land plants are also supported by geochemical and data. This is corresponding to Types I, II and II/III kerogen. Consequently, the Late Jurassic bituminous sediments are likely to be source rocks for mainly oil-generation.

3 Chemical results such as Tmax and PI suggest that the Late Jurassic bituminous shales in the Shabwah depression are in a low maturity stage, hence, they have not yet generated commercial oils, and considered to be unconventional oil shale.

4 The biomarker results presented in this study further indicate that the fine-grained shale sediments in the Shabwah depression were accumulated in a brackish marine under reducing environmental conditions. Such excellent conditions are favourable for a good preservation of organic matter that consequently enhanced organic richness in this high quality bituminous shale. The high concentrations of alginite (telalginite + lamalginite) and amorphous organic matter (AOM) further suggest sapropelite organic matter, depositing in marine reducing environmental conditions.

5 It is interesting to note that the shales of high TOC content >5% and high thickness of more than 200 m gave good criteria for significant unconventional exploration the Shabwah depression, and increase dramatically the conventional reserve across the Sabatayn Basin.

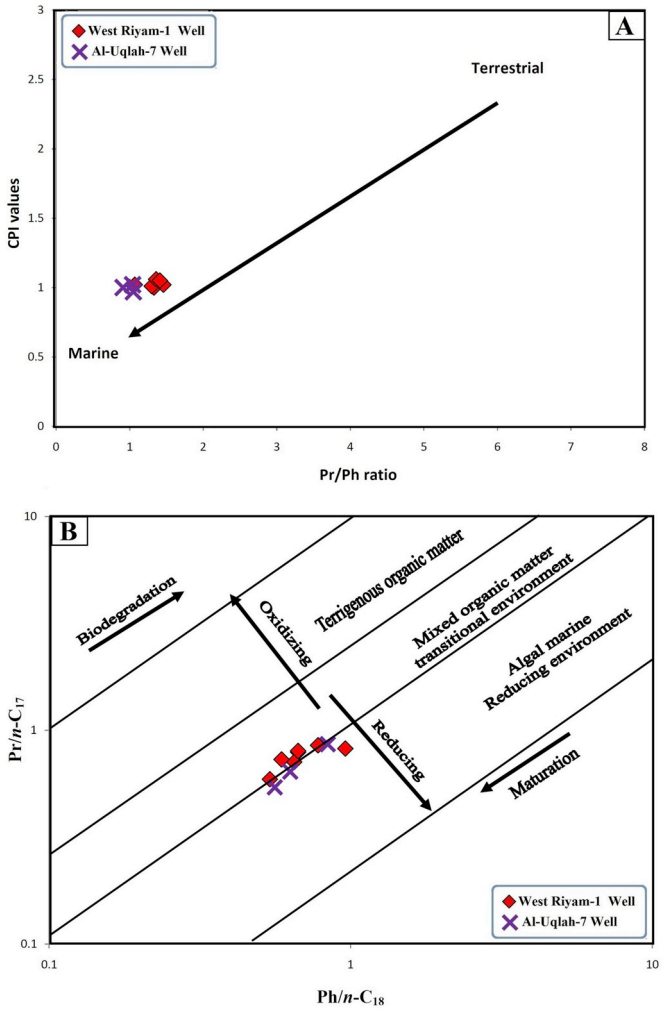

Fig. 10. Biomarker cross-plots of isoprenoid ratios and carbon preference indices (CPIs) for the analyzed bituminous shale samples.

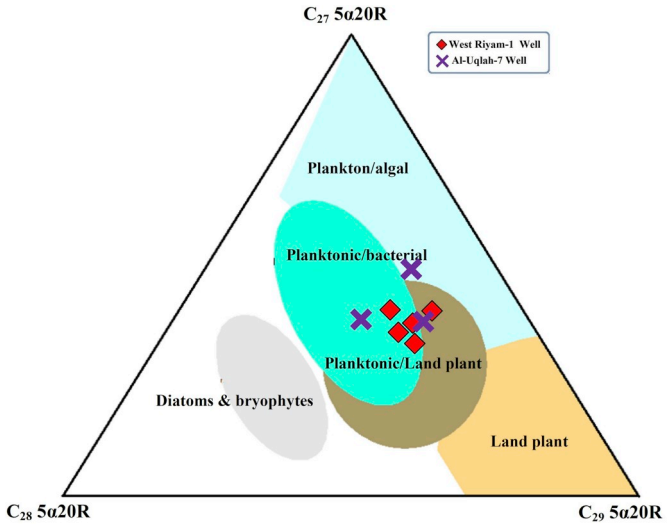

Fig. 11. Ternary diagram of regular steranes (C_{27}–C_{29}) indicating the relationship between sterane composition and organic matter input (modified after Huang and Meinschein, 1979).

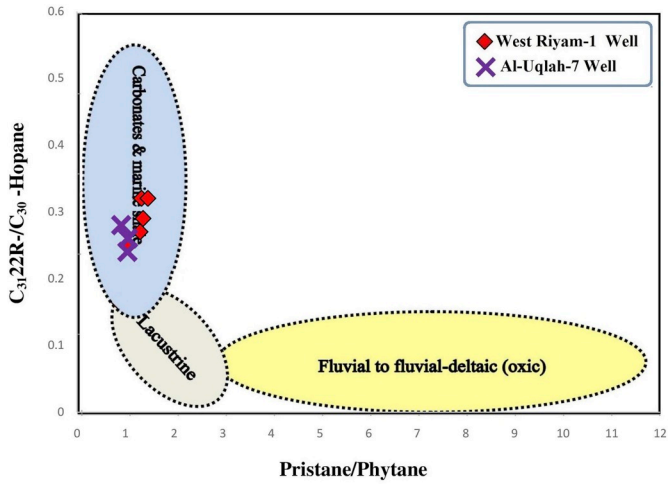

Fig. 12. Cross plot of hopane ratios versus pristane to phytane, showing marine depositional environment of the analyzed bituminous shale samples (modified after Peters et al., 2005).

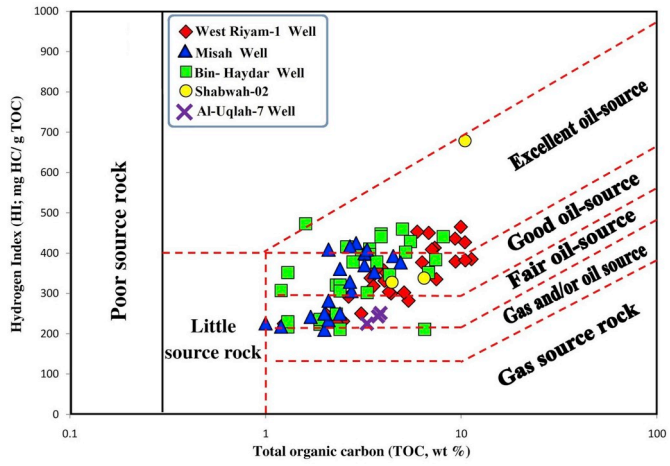

Fig. 13. Cross-plot of geochemical results of total organic carbon (TOC) content versus Hydrogen Index (HI), indicating that the analyzed bituminous shales are capable to generate mainly oil.

Author contributions section

Mohammed Hail Hakimi: Geological setting, analyses, interpretations, discussion and final writing, **Adel M. Al-Matary:** Geological setting, analyses, and draft writing, **Osama El-Mahdy:** Analyses, and draft writing, **Baleid Ali Hatem:** Collections the samples and analyses, **Ali Y. Kahal:** Writing and English Editing, **Aref Lashin:** Writing and English Editing.

Acknowledgements

Acknowledgements to the authority of Petroleum Exploration and Production (PEPA) in Yemen. The authors are also grateful to the Department of Geology at the University Malaya for providing organic geochemical facilities to complete this work. The authors extend their sincere appreciation to the Researchers Supporting Project number (RSP-2019/92), King Saud University, Riyadh, Saudi Arabia. The constructive comments by anonymous reviewers that improved the original article are gratefully acknowledged.

Appendix A. Supplementary data

Supplementary data to this article can be found online at https://doi.org/10.1016/j.petrol.2020.106951.

References

Abrams, M.A., Gong, C., Garnier, C., Sephton, M.A., 2017. A new thermal extraction protocol to evaluate liquid rich unconventional oil in place and in-situ fluid chemistry. Mar. Pet. Geol. 88, 659–675.

Al-Areeq, N.M., Al-Badani, M.A., Salman, A.H., Albaroot, M., 2018. Petroleum source rocks characterization and hydrocarbon generation of the upper Jurassic succession in Jabal Ayban field, Sabatayn Basin, Yemen. Egypt. J. Pet. 27, 835–851.

Alaug, A.S., Leythäeuser, D., Bruns, B., Ahmed, A.F., 2011. Source and reservoir rocks of the Block 18 oilfields, Sab'atayn Basin, Yemen: source rock evaluation, maturation, and reservoir characterization. Iran. J. Earth Sci. 3, 134–152.

As-Saruri, M.A., Sorkhabi, R., Baraba, R., 2010. Sedimentary basins of Yemen: their tectonic development and lithostratigraphic cover. Arab. J. Geosci. 3, 515–527.

Beydoun, Z.R., Al-Saruri, M., El-Nakhal, H., Al-Ganad, I.N., Baraba, R.S., Nani, A.S.O., 1998. International lexicon of stratigraphy. In: International Union of Geological Sciences and Ministry of Oil and Mineral Resources, second ed., vol. III. Republic of Yemen, Republic of Yemen; Publication 34, p. 245.

Brassell, S.C., Eglinton, G., Maxwell, J.R., Philp, R.P., 1978. Natural background of alkanes in the aquatic environment. In: Hutzinger, O., van Lelyveld, L.H., Zoeteman, B.C.J. (Eds.), Aquatic Pollutants: Transformation and Biological Effects. Pergamon, Oxford, pp. 69–86.

Brannin, J., Gurdip, S., Gerdes, K.D., Berry, J.A.L., 1999. Geological evolution of the central Marib-Shabwa basin. Yemen GeoArabia 4, 9–34.

Chandra, K., Mishra, C.S., Samanta, U., Gupta, A., Mehrotra, K.L., 1994. Correlation of different maturity parameters in the Ahmedabad–Mehsana block of the Cambay basin. Org. Geochem. 21, 313–321.

Cranwell, P.A., 1977. Organic geochemistry of Cam Loch (Sutherland) sediments. Chem. Geol. 20, 205–221.

Csato, I., Habib, A., Kiss, K., Kocz, I., Kovacs, V., Lorincz, K., Milota, K., 2001. Play concepts of oil exploration in Yemen. Oil Gas J. 99, 68–74.

Didyk, B.M., Simoneit, B.R.T., Brassell, S.C., Eglinton, G., 1978. Organic geochemical indicators of palaeoenvironmental conditions of sedimentation. Nature 272, 16–222.

Escobar, M., Márquez, G., Inciarte, S., Rojas, J., Esteves, I., Malandrino, G., 2011. The organic geochemistry of oil seeps from the Sierra de Perijá eastern foothills, Lake Maracaibo Basin, Venezuela. Org. Geochem. 42, 727–738.

Espitalié, J., Deroo, G., Marquis, F., 1985. La pyrolyse Rock-Eval et ses applications and developments Oil Gas. Sci. Technol. Rev. Inst. Fr. Pet. Energy Nouv. 40, 563–580.

Fatma, H., Sadettin, K., 2013. Organic geochemistry and depositional environments of Eocene coals in northern Anatolia Turkey. Fuel 113, 481–496.

Gürgey, K., 1999. Geochemical characteristics and thermal maturity of oils from the Thrace Basin (western Turkey) and western Turkmenistan. J. Pet. Geol. 22, 167–189.

Hakimi, M.H., Abdullah, W.H., 2013a. Organic geochemical characteristics and oil generating potential of the Upper Jurassic Safer shale sediments in the Marib-Shabowah Basin, western Yemen. Org. Geochem. 54, 115–124.

Hakimi, M.H., Abdullah, W.H., 2013b. Geochemical characteristics of some crude oils from Alif Field in the Marib-Shabowah Basin, and source-related types. Mar. Pet. Geol. 45, 304–314.

Hakimi, M.H., Abdullah, W.H., 2015. Thermal maturity history and petroleum generation modelling for the Upper Jurassic Madbi source rocks in the Marib-Shabowah Basin, western Yemen. Mar. Pet. Geol. 59, 202–216.

Hakimi, M.H., Ahmed, A.F., 2016. Petroleum generation modeling of the organic-rich shales of late Jurassic–early cretaceous succession from mintaq-01 well in the Wadi Hajar sub-basin, Yemen. Can. J. Earth Sci. 53, 1053–1072.

Hakimi, M.H., Abdullah, W.H., Shalaby, M.R., 2001. Organic geochemical characteristics and depositional environments of the Jurassic shales in the Masila Basin of Eastern Yemen. GeoArabia 16, 47–64.

Hakimi, M.H., Abdullah, W.H., Shalaby, M.R., 2012. Molecular composition and organic petrographic characterization of Madbi source rocks from the Kharir Oilfield of the Masila Basin (Yemen): palaeoenvironmental and maturity interpretation. Arab. J. Geosci. 5, 817–831.

Hakimi, M.H., Abdullah, W.H., Shalaby, M.R., Alramisy, G.A., 2014. Geochemistry and organic petrology study of Kimmeridgian organic-rich shales in the Marib-Shabowah Basin, Yemen: origin and implication for depositional environments and oil-generation potential. Mar. Pet. Geol. 50, 185–201.

Hakimi, M.H., Abdullah, W.H., Alqudah, M., Makeen, Y.M., Mustapha, K.A., 2016a. Organic geochemical and petrographic characteristics of the oil shales in the Lajjun area, Central Jordan: origin of organic matter input and preservation conditions. Fuel 181, 34–45.

Hakimi, M.H., Abdullah, W.H., Alqudah, M., Makeen, Y.M., Mustapha, K.A., 2016b. Reducing marine and warm climate conditions during the Late Cretaceous, and their influence on organic matter enrichment in the oil shale deposits of North Jordan. Int. J. Coal Geol. 165, 173–189.

Hakimi, M.H., Al-Matary, A.M., Hersi, O.S., 2018. Late Jurassic bituminous shales from Marib oilfields in the Sabatayn Basin (NW Yemen): geochemical and petrological analyses reveal oil-shale resource. Fuel 232, 530–542.

Hakimi, M.H., Alaug, A.S., Alramisy, G.A., Ahmed, A.F., 2019a. Petroleum that has migrated into an outcropping of the Jurassic Ayad Salt Dome of Shabwah depression, Yemen. Pet. Sci. Technol. 37, 296–304.

Hakimi, M.H., Alaug, A.S., Lashin, A.A., Mohialdeen, I.M.J., Yahy, M.M.A., Kinawy, M. M., 2019b. Geochemical and geological modeling of the Late Jurassic Meem Shale Member in the Al-Jawf sub-basin, Yemen: implications for regional oil and gas exploration. Mar. Pet. Geol. 105, 313–330.

Huang, W.Y., Meinschein, W.G., 1979. Sterols as ecological indicators. Geochem. Cosmochim. Acta 43, 739–745.

Hunt, J.M., 1996. Petroleum Geochemistry and Geology, second ed. W.H. Freeman and Company, New York.

Leventhal, J.S., 1987. Carbon and sulfur relationships in Devonian shales from the Appalachian basin as an indicator of environment of deposition. Am. J. Sci. 287, 33–49.

Makeen, Y.M., Abdullah, W.H., Hakimi, M.H., 2015. Source rock characteristics of the lower cretaceous Abu Gabra formation in the Muglad basin, Sudan, and its relevance to oil generation studies. Mar. Pet. Geol. 59, 505–516.

Mccarthy, K., Rojas, K., Niemann, M., Palmowski, D., Peters, K., Stankiewicz, A., 2011. Basic petroleum geochemistry for source rock evaluation. Oilfield Rev. 23, 32–43.

Merrill, R.K., 1991. Source and Migration Processes and Evaluation Techniques (Oklahoma).

Mohialdeen, I.M.J., Hakimi, M.H., 2016. Geochemical characterisation of Tithonian–Berriasian Chia Gara organic-rich rocks in northern Iraq with an emphasis on organic matter enrichment and the relationship to the bioproductivity and anoxia conditions. J. Asian Earth Sci. 116, 181–197.

Mukhopadhyay, P.K., Wade, J.A., Kruge, M.A., 1995. Organic facies and maturation of Jurassic/Cretaceous rocks, and possible oil-source rock correlation based on pyrolysis of asphaltenes, Scotion Basin, Canada. Org. Geochem. 22, 85–104.

Peters, K., Cassa, M., 1994. Applied source rock geochemistry. In: Magoon, L.B., Dow, W. G. (Eds.), The Petroleum System from Source to Trap, vol. 60. AAPG Memoir, pp. 93–117.

Peters, K.E., Walters, C.C., Moldowan, J.M., 2005. The Biomarker Guide: Biomarkers and Isotopes in Petroleum Exploration and Earth History, second ed., vol. 2. Cambridge University Press, Cambridge.

Philp, R.P., 1985. Biological markers in fossil fuel production. Mass Spectrom. Rev. 4, 1–54.

Redfern, P., Jones, J.A., 1995. The interior rifts of Yemen—701 analysis of basin structure and stratigraphy in a regional plate tectonic context. Basin Res. 7, 337–356.

SPT, 1994. The Petroleum Geology of the Sedimentary Basins of the Republic of Yemen, vols. 1–7. Unpublished Report.

Talbot, M.R., 1988. The origins of lacustrine oil source rocks: evidence from the lakes of tropical Africa. Geol. Soc. Lond. Spec. Publ. 40, 29–43.

Taylor, G.H., Teichmüller, M., Davis, A., 1998. Diessel CFK, Littke R, Robert P. Organic Petrology. Gebrüder Borntraeger, Stuttgart.

Tissot, B.P., Welte, D.H., 1984. Petroleum Formation and Occurrence, second ed. Springer Verlag, Berlin, p. 699.

Waples, D.W., Machihara, T., 1991. Biomarkers for geologists – a practical guide to the application of steranes and triterpanes in petroleum geology. Assoc. Pet. Geol. Methods Explor. 9, 91.